Appl. Phys. A 87, 385–389 (2007)
DOI: 10.1007/s00339-007-3915-y

**Applied Physics A**
**Materials Science & Processing**

M. MARISCAL[1]
E. LEIVA[1]
K. PÖTTING[2]
W. SCHMICKLER[2,✉]

# The structure of electrodeposits – a computer simulation study

[1] Unidad de Matematica y Fisica, Facultad de Ciencias Quimicas, Universidad Nacional de Cordoba, INFIQC, 5000 Cordoba, Argentina
[2] Department of Theoretical Chemistry, Universität Ulm, 89069 Ulm, Germany

**Received: 8 August 2006/Accepted: 11 December 2006**
**Published online: 9 March 2007 •** 

**ABSTRACT** A new method for the study of the molecular dynamics of electrochemical systems is presented, which explicitly contains the electrode potential. It is based on a combination of ordinary molecular dynamics, stochastic dynamics, and a grand-canonical ensemble. The method is tested for the deposition of silver on Au(111), and is found to represent the potential dependence of this process well. Application to the deposition of nickel on Au(111) reveals extensive surface alloying, while during the deposition of nickel on Pt(111) an atomic exchange between the two metals occurs only at step edges.

**PACS** 82.45.Qr; 71.15.Pd; 07.05.Tp

## 1 Introduction

The deposition of metal ions on an electrode surface is a fundamental process of electrochemistry. Before the advent of local probe techniques, the growth mechanism and the structure of the metal deposits could only be investigated by comparing current transients with the predictions of simple models. The information that could be gained in this way was limited, often uncertain, and in particular very little could be learned about the surface structure. With the advent of the scanning tunneling microscope (STM) and related methods the situation has improved substantially, and the structure of metal electrodes can now be imaged with atomic resolution. While these techniques have greatly improved our knowledge of the surface structure, they give only the location, but not the chemical nature of the imaged atom. This is particularly problematic in the case of the deposition of metal ions on a foreign metal substrate, where surface alloying may occur. In addition, the time resolution of the STM is low, and only processes which take place on the time scale of about one second, or a little longer, can be followed in real time, so that the dynamics of the surface can be investigated only in exceptional circumstances.

Much of the experimentally inaccessible information can in principle be obtained from computer simulations with large ensembles, provided the interaction potentials are sufficiently accurate. In this respect recent works employing embedded atom potentials have been quite encouraging. In particular, molecular dynamics simulations for the generation of metal clusters with the tip of an STM have explained the formation and the stability of the clusters [1, 2], and kinetic Monte Carlo simulations have permitted insight into the deposition of metals both at under- and overpotentials [3, 4]. For a detailed understanding of the kinetics of the deposition, molecular dynamics (MD) is the method of choice. Since the number of particles varies during the process, these simulations must be performed in a grand-canonical ensemble. However, the available variants of MD do not allow for a key factor: the electrode potential, which determines the free energy of the reaction, its rate, and even its direction – whether metal deposition or dissolution takes place. In addition, it would be desirable for the simulations to account for the presence of a depletion or accumulation layer in front of the electrode. In a recent publication [5] we have presented a new simulation method which achieves these goals, and reported on first applications to particular systems. In this work, we shall review this method, show how the electrode potential affects the rate and the structure of deposits and present some new results for systems that display surface alloying.

## 2 Simulation method

In order to make this paper self-contained, and to address a different audience, we briefly review our simulation method. The basic set-up of our simulation cell representing an electrochemical half cell is shown in Fig. 1; it consists of three principal parts. The bottom part, labelled A, contains six layers of metal atoms arranged in an fcc lattice containing 400 atoms per layer; the three bottom layers are kept fixed, the others are mobile and obey ordinary deterministic molecular dynamics. The interaction between these metal atoms are calculated from the embedded atom method [6]; the details have been given in our previous publication [5].

From the electrolyte solution, only the metal ions are modeled explicitly as particles contained in the regions B and C. In region C, which in the simulations reported here has a thickness of 12 Å, the concentration of the particles is kept constant by adding or removing particles, as required. In contrast, the region B, of height $L = 24$ Å, contains a variable number of particles and can thus represent a depletion layer for metal deposition. The particles in the solution do not interact with each other. Instead, they experience a constant background

✉ Fax: +49 731 502 2819, E-mail: Wolfgang.Schmickler@uni-ulm.de

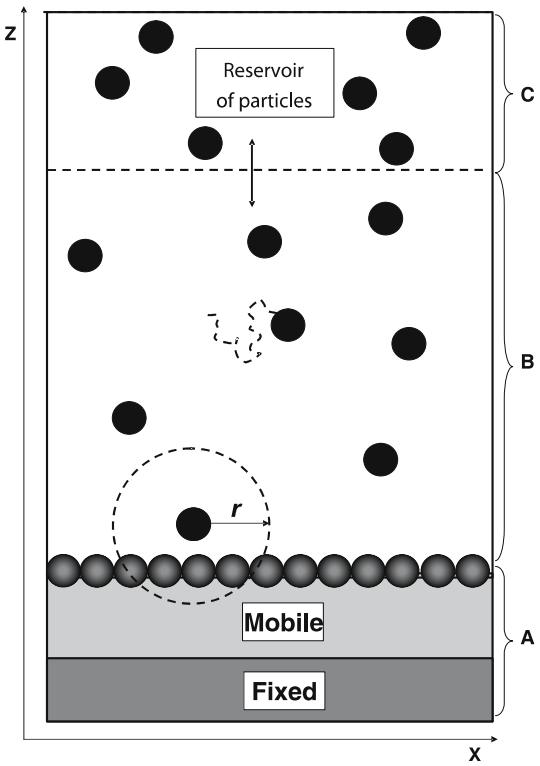


**FIGURE 1** Schematic representation of the simulation box

potential $\mu$ which, as we shall explain below, determines the effective electrode potential.

The solvent is represented indirectly as a thermal bath which induces stochastic motion in these regions. Thus, the particles in the solution obey Langevin dynamics according to:

$$\frac{\mathrm{d}v}{\mathrm{d}t} = -\boldsymbol{v}\gamma + \boldsymbol{F}_{\mathrm{R}} \tag{1}$$

where $\gamma$ is the friction constant and $\boldsymbol{F}_{\mathrm{R}}$ represents the random force acting on each particle. The friction constant $\gamma$ and the random force $\boldsymbol{F}_{\mathrm{R}}$ are related by the fluctuation–dissipation theorem. The Brownian dynamics were implemented by Ermak's algorithm [7].

The critical part is the interface between the regions A and B, where metal deposition or dissolution takes place. This was handled in the following way: at each time step the interaction potential $V_i$ of each particle $i$ in region B with the metal surface is calculated from the embedded atom method and compared with the background potential $\mu$. If $V_i < \mu$, the particle is deposited onto the surface. This means that the particle switches from Brownian to deterministic dynamics, keeping its velocity. The particle is then in the attractive part of the potential, so that backscattering is unlikely. Conversely, if a surface particle of metal M reaches the crossing point, where its potential energy equals the background potential $\mu$, it is dissolved and starts to obey Brownian dynamics.

By changing the background potential $\mu$ we change the driving force for metal deposition; raising $\mu$ increases the driving force. Let $\mu_0$ be the value at which deposition and dissolution are in equilibrium. Then the overpotential $\eta$ for the deposition is given by: $\mu - \mu_0 = -ze_0\eta$, where $z$ is the valency of the metal ion in the solution. Note that by convention a negative overpotential favors deposition. The equilibrium value $\mu = 0$ can be obtained from the condition that the kink sites of the electrode, whose energy is known within the embedded atom method, are in equilibrium with the solution; the entropy part of the free energy can be calculated from classical mechanics, and depends on the concentration of the particles in region C. In order to avoid misunderstandings associated with the electrochemical convention, we shall not specify overpotentials, but the background potential $\mu$ with respect to $\mu_0$, which is thus set to zero. Positive values of $\mu$ denote a driving force for deposition.

In the simulations reported the time step was set to 0.5 fs; in terms of this unit, the friction coefficient was set to $\gamma = 20$. The latter value was chosen such that the system is well thermalized, but not greatly slowed down by the friction.

## 3 Simulation results

We have applied our simulation method to a fair number of systems. Here we report first on the deposition of silver on Au(111). This process has been well investigated experimentally, and we have used this to check on the accuracy of our scale of electrode potential. We then proceed to present results for two systems which display surface alloying, viz. the deposition of nickel on Au(111) and Pt(111), but which differ in interesting details.

### 3.1 *Deposition of silver on* Au(111)

The deposition of silver on Au(111) has been well investigated experimentally, and we have therefore chosen it as a model system to investigate the potential dependence of the simulations. Deposition has been investigated both on flat surfaces (terraces) and on surfaces with an island. Silver and gold have almost the same lattice constants, so that there is no mismatch, and silver can be deposited on gold with little surface strain.

Ag on Au(111) is one of the systems which show a phenomenon known as underpotential deposition: up to a monolayer of Ag can be deposited at electrode potentials a little higher (remember the sign convention) than the deposition potential for silver on silver, indicating that at the surface the interaction of silver with gold is a little stronger than that of silver with itself. There have been a fair number of experimental studies of this process [8–13], which agree on the overall picture, but differ in details such as the onset potentials for the various deposition processes. They all agree that the deposition starts with the decoration of islands and steps at a potential of several hundred of mV below the equilibrium potential for bulk deposition. A monolayer is deposited at $\mu = -20$ meV, and at potentials above the equilibrium potential deposition occurs layer by layer, showing the familiar nucleation and growth phenomena.

In our simulations we observe the decoration of gold islands perimeters starting from $\mu = -246$ meV (see Fig. 2). This deposition stops when all gold edges accessible from kink sites have been filled. At $\mu = 64$ meV monolayers of silver are formed starting from the steps. The same phenomenon has been observed experimentally but at the slightly

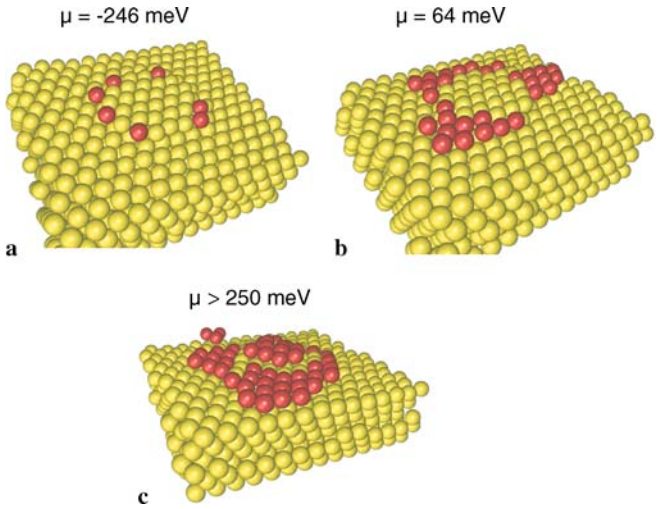


**FIGURE 2** Snapshots of silver deposition at an island on Au(111)

lower value corresponding to $\mu = -20$ meV already mentioned above. This discrepancy could either indicate a slight inaccuracy of our embedded atom potential, or a stabilization of the silver monolayer by anion adsorption, a phenomenon that often occurs. Our onset potential is also somewhat higher than the value of $\mu = -17$ mV predicted by Sanchez and Leiva [14] from ab initio calculations, or the value of $\mu = -50$ mV obtained by Oviedo et al. [15] using a slightly different version of the embedded atom potentials.

Within the timescale of our simulations deposition on flat terraces started at $\mu = 264$ meV; the delayed onset reflects the nucleation overpotential. This can be clearly seen from the corresponding curve in Fig. 3, which shows the number of deposited particles as a function of time. At short times, the number of deposited particles fluctuates around a critical cluster size of about 5–6 atoms. At higher potentials, nucleation is no longer observed, and the transients rise throughout. After the first layer has been completed, we observe layer by layer growth, in line with the experimental observations.

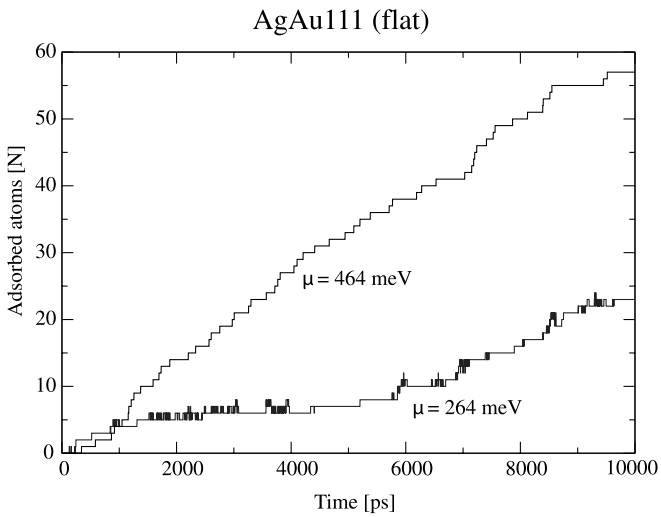


**FIGURE 3** Ag on Au(111) at $T = 300$ K. Number of atoms $N$ vs. time $t$ at two different potentials. The total number of places for Ag atoms on the surface is 196

In summary: our simulations for the deposition of silver on Au(111) show that our method works, and that the potential has an expected influence on the deposition rate. There may be a slight uncertainty in the potential scale, which could be caused by an inaccuracy of the interaction potential employed, or by the influence of anions on the experimental results.

### 3.2 *Deposition of* Ni *on* Au(111) *and* Pt(111)

Alloy formation during the deposition is of particular interest, because it is often suspected, but difficult to detect experimentally. Therefore we have examined the deposition of Ni on Au(111), where vacuum experiments have shown an exchange of the Ni atoms with the surface atoms of gold [16]. Subsequent deposition occurs with a layer by layer growth. Electrochemical deposition of Ni on Au(111) at overpotentials $\mu_0$ between 80 and 100 mV shows a nucleation and growth pattern very similar to that observed in ultra high vacuum (UHV) experiments [17].

Our simulations were performed in the diffusion-limited regime, in which all of the atoms that arrive at the surface are deposited, and none are dissolved. Figure 4 shows the final state after an amount equivalent to four Ni monolayers have been deposited. Ni and Au exchange very rapidly, and so Ni penetrates into the first few layers. In particular, the second layer consists almost totally of Ni atoms, while the top layer is rich in gold. Ni has a higher surface tension than gold, so that energy is gained if the nickel atoms are buried.

The high catalytic selectivity that Ni-Pt alloys have for certain reactions [18] make the Ni/Pt(111) system an interesting candidate for investigations. There are a fair number of electrochemical studies for this system, but they are mostly aimed at industrial conditions, and often use chloride electrolytes which are complicated by coadsorption [19]. In addition, nickel deposition is often accompanied by the parallel evolution of hydrogen; this could be avoided by using alkaline solutions [20], but there the purity of the solution poses a practical problem. Thus, a systematic investigation of the nature of the deposit, in particular, if alloy formation occurs, has not yet been undertaken, but is possible in principle. Our simulation therefore has predictive values.

We can compare our results with the final state of Ni deposition on platinum in the vacuum. Indeed, since alloy formation is governed by the interaction of the Ni atom with the substrate after the deposition, we may expect the final state to be quite similar for Ni deposition from solution and in UHV.

Gambardella et al. [21] have shown that Ni deposition on Pt(111) surfaces in UHV gives rise to the formation of stable metal alloys. They reported a favorable exchange of Ni atoms at step sites. Ni and Pt are known to form a continuous series of solid solutions in the bulk [22]. First principle calculations also show that Pt(111) has a surface energy lower than that of Ni(111) [23], and that Ni adatoms tend to diffuse into bulk Pt [24].

We have performed simulations on a Pt(111) surface with monoatomic steps called (open) and (closed) which have been generated by cutting a Pt(111) surface in the [100] and [110] directions respectively. In the case of closed steps the first stage of the Ni deposition starts by arrival of adatoms to the

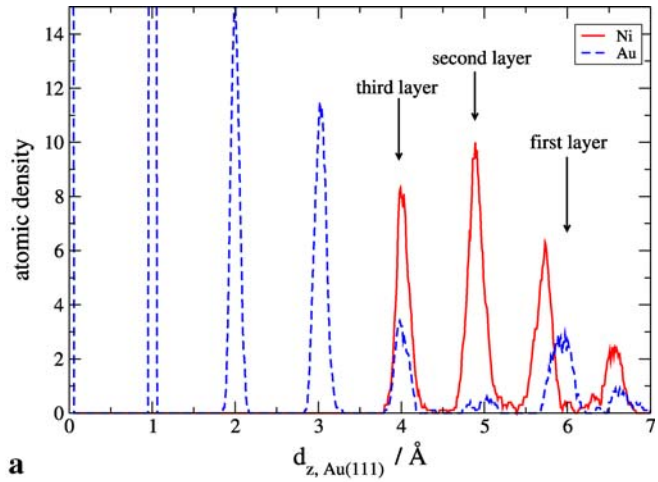


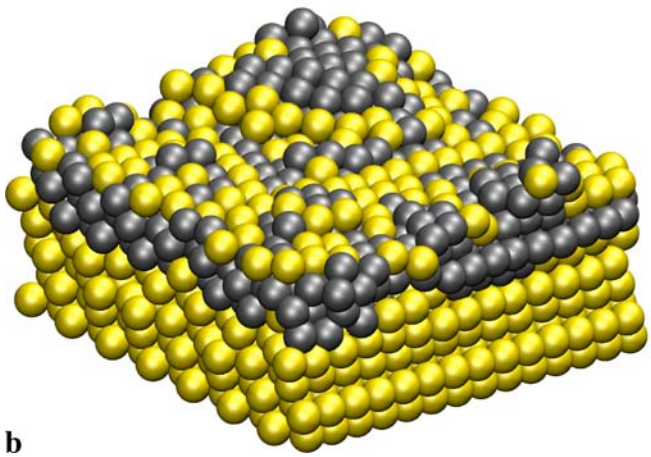


**FIGURE 4** Ni deposition on Au(111) with surface defects. (**a**) atomic density profile relative to the Au(111) interplanar distance, and (**b**) typical atomic configuration after deposition of Ni on Au(111)

flat surface and subsequent diffusion to the step edge. No exchange mechanism has been observed during the early stages. After the monoatomic steps are fully covered, Ni also starts to grow at the flat terraces. After completion of the first Ni overlayer about 9% of Pt atoms corresponding to step edges have been exchanged. In the case of more open steps deposition of Ni begins at step edges as well as at flat terraces. A very fast exchange diffusion mechanism is observed at the early stages, mainly at the steps. No mixing or exchange diffusion occurs at the flat terraces. The high coordination number that the open steps present could be one explanation for the differences found. After completion of four overlayers of Ni on Pt(111), exchange diffusion can be observed more clearly specifically at the step edges (Fig. 5). Very good agreement with experimental observations can therefore be noticed for the present system, indicating very fast diffusion mechanisms to form alloyed steps.

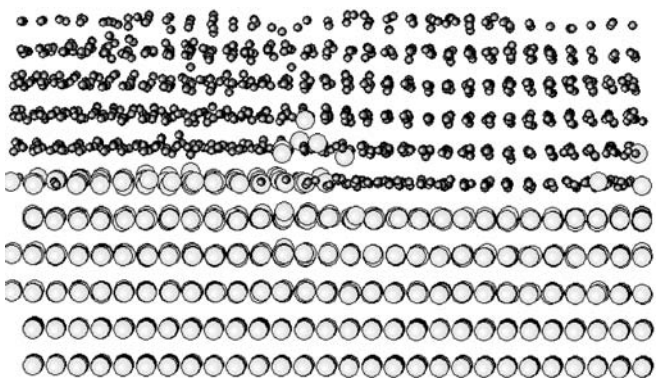

**FIGURE 5** Ni deposition on Pt(111) with an open step edge. The Ni atoms have been drawn much smaller in order to improve the clarity

## 4 Conclusions

The main new feature of our method is the inclusion of the electrode potential into molecular dynamics simulations. Judging from our first application, this seems to work well. In particular, the results for the deposition of Ag on Au(111) clearly show the decisive effect of the potential on the deposition rate, the formation of critical nuclei, and the structure of the deposit. The simulation for nickel deposition on Au(111) and Pt(111) clearly show the formation of a surface alloy in the former, and place exchange at edges in the latter case. At the present stage we have not included anions in the simulations. It is well known that in some cases the coadsorption of anions and metal cations leads to the formation of structures that resemble two-dimensional salts, and which form at potentials well below the deposition potential for the bulk metal. In principle, the inclusion of anions into our model should not present a major difficulty; one just needs reliable interaction potentials of the anions with the two metals involved, which could be obtained from ab initio calculations.

In our method, the solvent is only represented as a heat bath. Although an explicit inclusion of the solvent at a molecular level is possible, it would not yield any useful results. The ions in the solution would form solvation sheaths, which they would have to shed at least partially in order to be deposited. The required energy of activation is so high that no deposition could be observed during typical simulation times. This is a principle limitation of our method. As an alternative, kinetic Monte Carlo could be used, which yields, however, fewer details about the system dynamics.

**ACKNOWLEDGEMENTS** Financial support by the Landesstiftung Baden-Württemberg is gratefully acknowledged. E.P.M.L. would like to thank the program BID 1728/OC-AR PICT 06-12485 for support.

## REFERENCES

1 M.G. del Pópolo, E. Leiva, W. Schmickler, Angew. Chem. Int. Edit. **40**, 4674 (2001)
2 M.G. del Pópolo, E. P.M. Leiva, M. Mariscal, W. Schmickler, Nanotechnology **14**, 1009 (2003)
3 M.C. Gimenez, M.G. del Pópolo, E.P.M. Leiva, Langmuir **18**, 9087 (2002)
4 M.C. Gimenez, M.G. del Pópolo, E.P.M. Leiva, S.G. Garcia, D.R. Salinas, C.E. Mayer, W.J. Lorenz, J. Electrochem. Soc. **149**, 1 (2002)
5 K. Pötting, M. Mariscal, W. Schmickler, Chem. Phys. **320**, 149 (2006)
6 S.M. Foiles, M.I. Baskes, M.S. Daw, Phys. Rev. B **33**, 7983 (1986)
7 M.P. Allen, D.J. Tildesley, *Computer Simulation of Liquids* (Charendon Press, Oxford, 1987)
8 M.J. Esplandiu, M.A. Schneeweiss, D.M. Kolb, Phys. Chem. Chem. Phys. **1**, 4847 (1999)
9 T. Hachiya, K. Itaya, Ultramicroscopy **42**, 445 (1992)
10 K. Ogaki, K. Itaya, Electrochim. Acta **40**, 1249 (1995)
11 S. Garcia, D. Salinas, C. Mayer, E. Schmidt, G. Staikov, W.J. Lorenz, Electrochim. Acta **43**, 3007 (1998)

12 S.G. Corcoran, S.G. Chakarova, K. Sieradzki, J. Electroanal. Chem. **33**, 85 (1994)
13 S.G. Corcoran, S.G. Chakarova, K. Sieradzki, Phys. Rev. Lett. **71**, 1585 (1993)
14 C. Sanchez, E.P.M. Leiva, J. Electroanal. Chem. **458**, 183 (1998)
15 O. Oviedo, E.P.M. Leiva, M.I. Rojas, Electrochim. Acta **51**, 3526 (2006)
16 F.A. Möller, O. M. Magnussen, R.J. Behm, Phys. Rev. Lett. **77**, 5249 (1996)
17 O.M. Magnussen, R.J. Behm, J. Electroanal. Chem. **467**, 258 (1999)
18 Y. Gauthier, R. Baudoing, Y. Joly, R. Rundgren, J.C. Bertolini, J. Massardier, Surf. Sci. **162**, 342 (1985)
19 E. Gomez, R. Pollina, E. Vallez, J. Electroanal. Chem. **386**, 45 (1995)
20 M. Chatenet, R. Faure, Y. Soldo-Olivier, J. Electroanal. Chem. **580**, 275 (2005)
21 P. Gambardella, K. Kern, Surf. Sci. Lett. **475**, L229 (2001)
22 M. Hansen, *Constitution of Binary Alloys*, 2nd edn. (McGraw-Hill, New York, 1958)
23 I.A. Abrikosov, A.V. Ruban, H.L. Skriver, B. Johansson, Phys. Rev. B **50**, 2039 (1994)
24 A. Christensen, A.V. Ruban, P. Stoltze, K.W. Jacobsen, H.L. Skriver, J.K. Nørskov, F. Besenbacher, Phys. Rev. B **56**, 5822 (1997)